THE ISENTROPIC COMPRESSIBILTY OF ALUMINUM, COPPER, LEAD, AND IRON AT HIGH PRESSURES

L. V. AL'TSHULER, S. B. KORMER, M. I. BRAZHNIK, L. A. VLADIMIROV, M. P. SPERANSKAYA, and A. I. FUNTIKOV

Submitted to JETP editor October 7, 1959; resubmitted January 3, 1960

J. Exptl. Theoret. Phys. (U.S.S.R.) **38**, 1061-1073 (April, 1960)

A method is described for measuring the speed of propagation of weak disturbances behind the front of strong shock waves. The existence of two sound velocities, corresponding to the elastic and plastic states of the material, has been detected. With the aid of the techniques which have been developed, the sound velocities and isentropic compression moduli of aluminum, copper, iron, and lead have been determined in the pressure range 0.4 to 3.5×10^6 atmos. On the basis of the experimental results so obtained, the magnitudes of the thermal energy, the temperatures of the shock compression, and the Gruneisen coefficients have been estimated.

INTRODUCTION

THE new methods of studying the properties of matter at high pressures are based on the use of strong shock waves.[1,2] A determination of two of the wave parameters — its velocity of propagation and the velocity of the mass of material behind the front — permits the pressure and density in the shock compression to be found.

A third important kinematic parameter of a shock wave is the speed of sound within the material compressed by the shock. Its value characterizes the speed with which small disturbances (weak shocks and relaxation waves) are propagated through the compressed material. A knowledge of the speed of sound, in this sense, is of undoubted interest, not only for geophysical investigations, but also for other investigations connected with the propagation of sound and shock waves, and in particular for properly setting up experiments to determine dynamic compressibility.

Measurements of sound velocity play a large part in the study of the equation of state. It is well known that a shock compression increases the internal energy of a body by the amount $\Delta E = \frac{1}{2}P_\Gamma(v_0 - v)$, where P_Γ is the pressure in the shock, v_0 is the initial specific volume, and v is the specific volume behind the shock wave front. On the diagram of pressure vs specific volume (Fig. 1), ΔE is equal to the area of the triangle OAB. The energy thus acquired is partly spent in overcoming the elastic repulsive forces, increasing the elastic potential of the lattice by an amount equal to the area of the curvilinear triangle O_1DA.

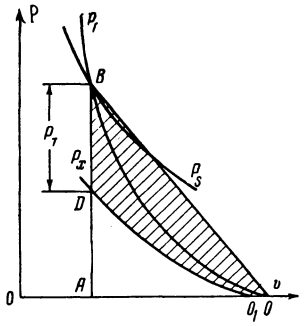

FIG. 1

The remaining part, represented by the shaded area in the diagram, is liberated in the form of thermal energy, heating up the material and increasing its entropy. As a result, the points on the dynamic adiabatic lie on different isentropics P_S above the curve for elastic or cold compression P_X. Through the relation $-v^2(\partial P/\partial v)_S = C^2$, measurements of the speed of sound behind the front of a strong shock wave determine the slope of the isentropics — in other words, the isentropic compressibility of the material — in the extreme high pressure region of hundreds of thousands or millions of atmospheres.

In the present study we present methods of measuring the speed of sound behind the front of strong shock waves, and the results of measurements on aluminum, copper, lead, and iron in the range of pressure from 4×10^5 to 3.5×10^6 atmos. On the basis of the experimental results obtained, the isentropic derivatives have been calculated and the thermal energies and temperatures in the shock have been estimated. The Grüneisen coefficients have also been estimated, with somewhat less accuracy.

1. MEASUREMENTS OF THE SPEED OF SOUND BY THE LATERAL RELAXATION METHOD

By definition, the speed of sound is the speed of propagation of small disturbances with respect to the moving material. Since at the wave front $C + U > D$ (U being the bulk velocity of the material behind the shock wave front and D the velocity of the front), it follows that any disturbance originating behind the shock wave front will overtake the front, and will produce changes in all the parameters, including the kinematic parameters U and D themselves. This permits measurements to be made of the velocity of propagation of acoustic disturbances, since it registers their arrival at the shock wave front.

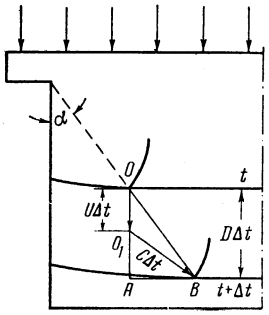

FIG. 2

In the method of lateral relaxation, the shock wave moves along a cylindrical sample with a stepped shape (Fig. 2). The surface of the shoulder acts as a source of rarefaction waves. Expansion waves propagate with the speed of sound through the shock in the metal and overtake the shock wave front, causing a reduction of pressure in the peripheral zone of the sample.

Let us consider the two positions of the shock wave front at the instants t and $t + \Delta t$. Let the point O separate the relaxed portion of the front from the unrelaxed part. After the time Δt the shock wave has progressed a distance $D\Delta t$, and the metal particles which were originally at point O have been displaced along behind the front for a distance $U\Delta t$. After the same interval Δt the relaxation waves will have reached a sphere of radius $C\Delta t$ with its center at O_1. Since the motion of the rarefaction waves caused when a shock wave passes around an internal angle is self similar, the trajectory of the boundary point is a straight line, making a constant angle of relaxation α with the direction of propagation of the shock wave. In the right-angled triangle O_1AB we have $AB = \sqrt{(C\Delta t)^2 - (D-U)^2\Delta t^2}$. The same leg in the triangle AOB is $AB = D\Delta t \tan\alpha$. Equating, we obtain the following expressions for the tangent of the relaxation angle and the speed of sound:

$$\tan\alpha = \sqrt{(C/D)^2 - [(D-U)/D]^2}, \quad (1)$$

$$C = D\sqrt{(\tan\alpha)^2 + [(D-U)/D]^2}. \quad (2)$$

Thus, for measurements of the speed of sound by the lateral relaxation method, if the parameters D and U for the shock wave are known, the tangent of the relaxation angle α must be determined experimentally.

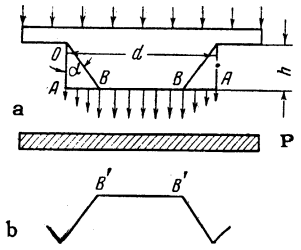

FIG. 3. a – Scheme of experiment for determining the relaxation angle. b – Front of the flying material.

The general scheme of the experiment for measuring the angle α is evident from Fig. 3. Until the instant when the shock wave emerges from the sample slab, the relaxation waves create a region of reduced pressures and lower throw-off speeds on the wave-front surface. The velocity of the free surface of the sample therefore falls off from point B toward point A, as shown schematically by the lengths of the arrows. The boundary of the unrelaxed region is found by measuring the throw-off velocities, or (which amounts to the same thing) the difference in the time of flight of the metal to a Plexiglas plate P fixed a short distance away from the sample. The process of the collision of the thrown-off surface with the Plexiglas surface is determined with a double-objective slit photo-chronograph with a type SFR-3 rotating mirror[3] having a sweep speed up to 6 km/sec. A break in the profile of the flying material (see points B′ in the sketch of the photochronogram, Fig. 3) determines the boundary of the unrelaxed region. Knowing the diameter of the shoulder d, the height h of the sample, the scale of the photograph k, and the distance B′B′ measured on the film, we find the quantity of interest to us from the formula

$$\tan\alpha = (d - kB'B')/2h. \quad (3)$$

where k is the ratio of the dimensions in nature to the dimensions on the film.

The shock wave parameters necessary to evaluate the speed of sound from (2) are determined in separate experiments. If the dynamic adiabatic is known, it is sufficient to measure a single parameter of the shock wave, for example its velocity D.

2. RELAXATION WAVES – ELASTIC AND PLASTIC

At pressures of 300 to 500×10^3 atmos, the photochronograms recording the time differences in the shock along the indicator surface differ fundamen-

tally in nature for materials having different mechanical properties. With water, for example, the photograph records a sharp bend at the boundary of the unrelaxed zone (see Fig. 4a). On the other hand, with a steel sample the curve has a rounded contour without sharply defined boundaries to mark off the region of the relaxation waves (Fig. 4b).

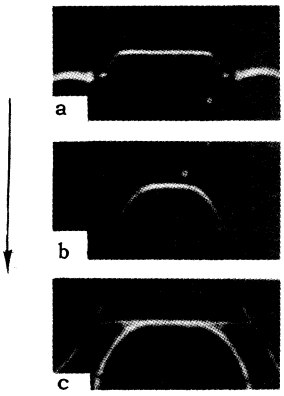

FIG. 4. Experimental photochronograms. Velocity of travel of the light across the film is 6 mm/microsec. Direction of motion is shown by the arrow.

On the basis of the pictures obtained, it can be assumed that for rigid materials the more slowly moving particles of the peripheral zone retard the neighboring portions of the unrelaxed region, which originally received the maximum momentum. In practice, if a thin layer of water or alcohol is applied to the metal surface to receive the momentum of the free surface, it permits the distribution of velocities across the sample diameter to be recorded more clearly, and the boundary of the unrelaxed zone to be determined with high precision (see Fig. 4c). Nonetheless, the difference in flight time for different parts of the liquid layer confirms in basic outline the picture derived above of a gradual decrease of velocity in the relaxed zone, and a large relaxation angle.

Table I gives the results of relaxation angle measurements for water, copper, and iron at relatively small shock pressures. The sound velocities C^* and the corresponding compressibility moduli $\rho_0 C^{*2}$ have been calculated from the observed relaxation angles. In Table I these quantities are compared with the values of the derivatives of the dynamic adiabats $dP_\Gamma/d\sigma$, which for low pressures characterize the isentropic compressibilities of the materials with reasonable accuracy. For water the experimentally measured modulus $\rho_0 C^{*2}$ is somewhat smaller than the derivative of the dynamic adiabat, in agreement with the theory of the subject; for copper and iron it is considerably greater — approximately 1.5 times.

The data given in the table prove beyond doubt that in the metals under consideration there are wave systems propagating with speeds greatly exceeding the isentropic velocity of acoustic waves of volume compression.

In order to understand their origin, let us consider the variation in the state of stress of a metal which has been compressed by a shock wave, when a plane relaxation wave acts upon it. The elastoplastic properties of an isotropic medium are characterized by three constants: the Young's modulus E, the Poisson ratio μ, and the critical shear stress σ_k. Under the influence of the relaxation wave the compressive stress in the direction normal to the relaxation front decreases by some amount ΔP_n, and in a direction parallel to the front it decreases by ΔP_τ. From the symmetry conditions in the planes parallel to the relaxation front, two of the principal stresses are equal, and there will be no deformation parallel to the front. This condition leads to the identity

$$\Delta P_\tau - \mu(\Delta P_\tau + \Delta P_n) = 0,$$

which enables us to connect the intensity of the relaxation wave

$$\Delta P_n = [(1-\mu)/(1-2\mu)](\Delta P_n - \Delta P_\tau)$$

with the difference between the principal stresses. As long as

$$\Delta P_n \leqslant [(1-\mu)/(1-2\mu)]\, 2\sigma_k,$$

the medium behaves like an elastic body, with a velocity of propation for longitudinal elastic waves $C^* = \sqrt{(K_S + \frac{4}{3}G)/\rho}$. In this expression, $K_S = E/3(1-2\mu)$ is the isentropic modulus of volume compression, and $G = E/2(1+\mu)$ is the shear modulus. When

$$\Delta P_n > [(1-\mu)/(1-2\mu)]\, 2|\sigma_k|$$

the medium changes to a state of plastic flow, for which the shear modulus is taken to be zero. Under these conditions the speed of the "plastic" relaxation waves $C = \sqrt{K/\rho}$, just as in the case of

TABLE I

Material	α, deg	D, km/sec	U, km/sec	C^*, km/sec	$\rho_0 C^{*2}$, 10^{10} d/cm^2	$dP_\Gamma/d\sigma$, 10^{10} d/cm^2	μ	ν
Water	47.5	4.42	1.52	5.60	31.4	34.2	—	—
Copper	41	5.24	0.87	6.33	357.8	288.8	0.34	0.82
Iron	46.5	5.34	0.98	7.15	401.3	298.2	0.28	0.77

liquids, is determined by the isentropic modulus of volume compression K_S. The velocity ratio

$$C/C^* = \nu = \sqrt{(1+\mu)/3(1-\mu)}. \quad (4)$$

depends only on the Poisson ratio.

The existence of two speeds, "elastic" and "plastic," under the experimental conditions of Fig. 3 leads to the appearance of two concentric zones of relaxation on the wave front surface — an inner "elastic" zone of weak relaxation and an external "plastic" zone.

Making use of the relation (4), we can calculate from C^* the value of the isentropic modulus $K_S = \rho_0 C^2 = \rho_0 C^{*2}\nu^2$. For both metals the values so obtained, $K_S \approx 240 \times 10^{10}$ d/cm^2, are somewhat smaller than $dP_\Gamma/d\sigma$, confirming the theory proposed above for the phenomenon.

The elastic relaxation zone is weakly developed in materials such as lead which have a large Poisson ratio and a small value of critical shear stress. Because σ_k decreases with temperature, it would seem at first sight that the high temperatures in a strong shock should lead to the disappearance of the elastic relaxation wave for all materials. However, this is countered by the high pressures, which increase the melting temperature[4] and raise the critical shear stress. Thus, according to Bridgman's data,[5] the application of pressures of 25×10^3 and 50×10^3 atmos increases $2\sigma_k$ for soft iron from 1200 kg/cm^2 to 6600 and 12000 kg/cm^2 respectively. For copper at these pressures $2\sigma_k$ is equal to 1050, 3000, and 4900 kg/cm^2 respectively. In view of these statements, it is quite possible that longitudinal elastic waves will exist at shock pressures of 10^6 atmos and above.

In relation to the method, the presence of an elastic zone makes the accurate determination of the boundary of the "plastic" relaxation much more difficult. The method described in the following section does not have this drawback.

3. THE OVERTAKING-RELAXATION METHOD

In the overtaking-relaxation method we study the collision between a plate and a sample, made of materials with known dynamic adiabats. In the simplest variant of the method, the plate and sample are made of the same material. From the surface of impact, shock waves OB and OA travel through the sample and the moving plate (see the x, t diagram, Fig. 5). At the instant the shock wave emerges from the rear surface of the plate (point A) a centered rarefaction wave is set up which overtakes the shock wave and weakens it. The occurrence of the first α-characteristic on the shock wave trajectory takes place at a distance

$$l = [(1+M)/(1-M)]\,\Delta, \quad (5)$$

where Δ is the thickness of the striker plate and $M = (D-U)/C$ is the Mach number. The relation (5) enables one to find M, provided that there actually is an overtaking, and consequently to find C also, if $D_1 - U_1$ is known. This form of the method was proposed by E. I. Zababakhin in 1948.

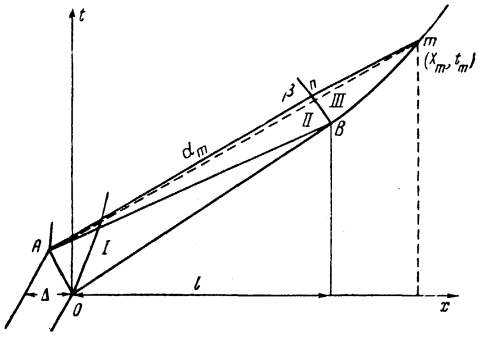

FIG. 5

Since the determination of the distance l, where the wave begins to slow down because of the presence of the faster elastic relaxation wave, is beset with considerable experimental error, it is expedient to change the form of the method and find the time t_m of arrival of the shock wave at a given point m, already known to lie on the relaxed portion of the shock wave trajectory. In this way one finds the slope of the α-characteristic $W_{\alpha m} = U_m + C_m$ that passes through the origin of the x, t diagram and the point m, whose coordinates are x_m and t_m. Then by measuring the material velocity U_m at the same point directly, or by determining it from a known shock adiabatic equation, we find the velocity of sound $C_m = W_{\alpha m} - U_m$ from the speed of the shock wave. In an expanded form, it is not difficult to show that

$$C_m = \frac{x_m + (2-\sigma_1)\,\Delta/\sigma_1}{D_1 t_m - \Delta} D_1 - U_m, \quad (6)$$

where $\sigma_1 = D_1/(D_1 - U_1)$ and D_1 are the parameters for the unrelaxed region.

Thus, the measurement of the velocity of sound by the overtaking-relaxation method reduces to the experimental determination of the shock wave trajectory in x, t coordinates, plus a measurement of the material velocity at one or a number of points on this trajectory.

The whole of the above treatment is valid under the assumption that the α-characteristics are straight lines everywhere in the region OAm, with a slope $W_a = U + C = \text{const}$. Let us go into this question in more detail. When two similar materials collide, three regions of flow can be distinguished in the x, t plane (see Fig. 5): I — the region OAB; II — ABn; and III — Bnm. In regions

I and II the flow is isentropic, since in region I the value of W_α is constant over the whole region, and in II it is constant over each α-characteristic. In region III the flow is not isentropic, since the intensity of the shock wave (and consequently also the entropy of the material behind its front) decreases beyond the point B, where the relaxation wave traveling from point A first overtakes the shock wave front. Here, in contrast to region II, the Riemann invariant β is not constant, and consequently W_α is not constant either.

Having determined the velocity of sound at the point m by the method outlined above, we then approximate the characteristic Anm by the straight line Am, introducing thereby a certain inaccuracy. In order to estimate the error, some numerical calculations have been made of the motion of a decaying shock wave in an aluminum test piece. In this calculation the equation of state

$$P - P_x = (n-1)v^{-1}(E - E_x), \qquad P_x = a[(v_0/v)^n - 1],$$

was used, taking into account not only the elastic terms but also the thermal terms in the pressure and energy. Different values of n from 1.67 to 4 were used in the computations, corresponding to a variation of the Grüneisen coefficient from $\frac{2}{3}$ to 3.

The calculations showed that in aluminum at plastic shock velocities of 5.6 km/sec, at distances of ten or more times the thickness of the plate, the maximum error in the sound velocity did not exceed 1.5%. At this point the pressure at the front of a decaying wave amounts to about one half of its original value. The error is smaller the closer the measuring region is to the portion of the shock wave not reached by the relaxation. A similar calculation has also been carried out for lead with the same results, using the equation of state taken from reference 6.

For a collision between plates of unlike materials, we must know not only the shock adiabatic for the striker plate but also the relation between the material velocity and the sound velocity in the rarefaction wave. In this case the computation of results is somewhat more complicated, since at the collision boundary there is a discontinuity at which the α-characteristics are refracted as they pass.

There are two possible cases of collision: when the material of the test piece is "softer" and when it is "harder" than the material of the striker plate. By the terms "softer" and "harder" we mean a flatter or steeper slope of the Hugoniot adiabat for the given material in P, U coordinates. In both cases the refraction of the α-characteristics can easily be taken into account with the aid of the x, t and P, U diagrams.

4. EXPERIMENTAL RESULTS

A determination of the speed of sound behind the front of strong shock waves presupposes a knowledge of the dynamic adiabats. In working out the experimental data of the present investigation, the dynamic adiabats given in reference 6 for aluminum, copper, lead, and iron were used.

In the first series of experiments the decay curves of shock waves were recorded in test pieces of aluminum, copper, lead, and iron when struck by a 2 mm aluminum plate. The speed of the plate was 5.60 km/sec. In order to record the trajectory of the shock wave in the test piece, which was made up of several plates, electrical contact pickups were introduced through small drill-holes. The successive short-circuiting of the pickups by the shock wave was recorded on a single-sweep cathode ray oscillograph. The

TABLE II

Metal	D_{Al}, km/sec	x_m, mm	t_m, msec	D_m, km/sec	P_m, 10^{10} d/cm^2	σ_m	C_m, km/sec
Aluminum	9,13	—	—	9,13*	69,3*	1,442*	—
		14,20	1,558	8,52	54,5	1,383	8,84
		19,16	2,205	7,92	41,2	1,320	8,13
Copper	10,45	—	—	6,69*	108,7*	1,374*	—
		10,95	1,697	5,92	69,2	1,284	6,32
		14,94	2,399	5,54	52,4	1,237	5,95
Lead	10,34	—	—	4,91*	105,2*	1,626*	—
		6,47	1,373	4,16	65,6	1,502	4,24
		9,45	2,133	3,72	46,4	1,420	3,85
Iron	10,31	—	—	7,01*	104,5*	1,374*	—
		10,93	1,656	5,76	54,2	1,263	6,70
		14,90	2,374	5,34	41,5	1,228	6,12

*The marked states are in the unrelaxed region.

TABLE III

Metal	D_{Fe}, km/sec	x_m, mm	t_m, msec	U_m, km/sec	P_m, 10^{10} d/cm^2	σ_m	C_m, km/sec
Aluminum		—	—	3.77*	107.2*	1.561*	—
	7.06	12.50	1.194	3.54	97.5	1.534	9.76
		—	—	2.77*	200.6*	1.519*	—
	8.67	8.00	0.992	2.47	169.2	1.475	7.78
Copper		11.00	1.398	2.12	135.2	1.422	7.13
		15.00	1.981	1.77	104.6	1.365	6.71
		—	—	2.82*	197.3*	1.842*	—
	8.61	6.00	0.988	2.34	146.7	1.734	5.16
Lead		9.00	1.572	1.84	100.8	1.616	4.62
		12.00	2.225	1.56	78.0	1.545	4.29
		—	—	2.86*	191.4*	1.502*	—
	8.54	8.00	0.940	2.62	168.0	1.472	8.49
Iron		11.0	1.329	2.12	122.3	1.405	7.85

*See footnote to Table II.

states in the striker plate and in the first thin screening plate were found graphically, from the intersection of the Hugoniot adiabat for aluminum with the adiabatic for the test piece on the pressure-velocity diagram. From the time delays found experimentally and the distance between the pickups, the trajectory of the shock wave was constructed and the wave velocities in the different portions of the trajectory were determined. In each experiment the recording was carried out over several base-lines.

The results of the measurements are given in Table II. Here t_m is the time from the instant of collision, and x_m is the distance from the collision surface. In the second column of the table are shown the speeds of the shock waves passing through the aluminum plate after the collision.

In the second series of experiments the amplitude of the unrelaxed wave was increased to 1.0 $\times 10^6$ atmos for aluminum and to 1.8×10^6 atmos for the other metals. A 1.5-mm steel plate was used as the striker, moving at 5.71 km/sec. In order to make the decay curves observable, a thin aluminum film was applied to the surface of the test piece parallel to the collision surface. When the shock wave emerged at the boundary of the film and the test piece, the film was torn away from the test piece and was projected with a velocity W_{Al} characterizing the amplitude of the wave at that cross section of the sample. The time (and consequently also the velocity with which the film moved) was recorded on a velocity photochronograph by the illumination from the shock wave in the air. The illumination was produced at the instant of the first movement of the film, and stopped as soon as it collided with a Plexiglas barrier, placed at a distance of 8 — 12 mm from the test sample. The transition from the speeds of motion of the aluminum film to the material velocities behind the shock wave front was accomplished with the aid of special calibrating experiments, in which measurements were made of the velocity acquired by an aluminum film under the influence of shock waves of known amplitudes. The decay curves U(x) for the four metals under investigation are shown in Fig. 6, together with the

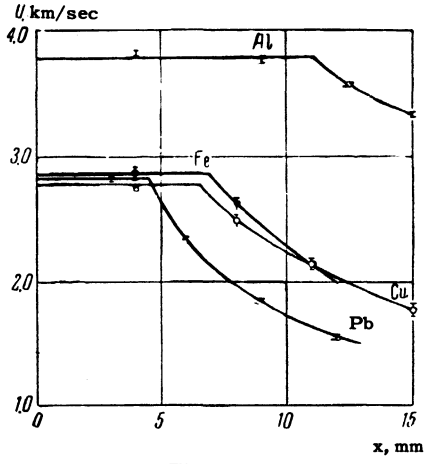

FIG. 6

experimental reference points. A knowledge of the U(x) curve makes it possible, with the aid of the known D, U relationships, to proceed successively to the D(x) curve and the curve $t(x) = \int_0^x dx/D$. The subsequent treatment of the experiment in the second series was identical with the treatment of the experiments in the first series. The results so obtained are shown in Table III.

The chief difference in the experiments of the third series (Table IV) consisted in a further increase of the projection velocity of the steel striker. Here the speed of sound was measured at pressures exceeding 1.5×10^6 atmos for aluminum and 3.5×10^6 atmos for copper, lead, and iron.

TABLE IV

Metal	P_m, 10^{10}d/cm^2	σ_m	C_m, km/sec
Aluminum	195.5	1.761	11.74
	160.0	1.701	11.23
Copper	379.6	1.694	9.48
	311.7	1.638	8.93
Lead	385.0	2.177	6.56
	279.5	2.003	5.92
Iron	347.8	1.650	9.98
	284.9	1.600	9.53

The experimental values of the sound velocities made it possible to find the dependence of the Mach number, $(D-U)/C$, and the tangent of the relaxation angle, $\tan\alpha$, on the degree of compression. The Mach number, as is well known, expresses the relative velocity of the relaxation wave and the shock wave. In its turn, $\tan\alpha$ defines the region of the shock wave which has been reached by the relaxation wave produced when the wave front meets a source of perturbation. Both these quantities can be calculated either from the propagation velocity C of the compressional waves, or from the velocity C* of longitudinal elastic waves. In this connection,

$$M^* = \nu M, \qquad \tan\alpha^* = [\nu^{-2}\tan^2\alpha + \sigma^{-2}(\nu^{-2}-1)]^{1/2}.$$

Note that when $\sigma = 1$ the magnitude of $\tan\alpha^*$ is finite and equal to $\sqrt{2(1-2\mu)/(1+\mu)}$, whereas $\tan\alpha$ drops to zero when $\sigma = 1$.

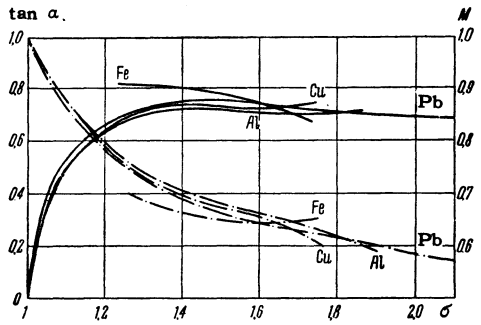

FIG. 7. Dependence of Mach number (dot-dash curves) and tan α (full curves) on the degree of compression.

Figure 7 shows the experimental values of M and $\tan\alpha$ for the four metals. The values of $\tan\alpha$ for very high pressures lie in an extremely narrow interval from 0.66 to 0.73, regardless of the fact that these metals have different compressibilities. Even more striking is the fact that the same values of $\tan\alpha$ at high values of compression are also possessed by water, paraffin, and Plexiglas, according to measurements by the authors. Apparently it is possible to use the value $\tan\alpha \approx 0.7$ for very strong shocks waves in other materials also.

It is essential to know the values of the Mach numbers and relaxation angles in order to set up experiments for investigation of dynamic compressibilities in a proper manner. It has been shown above that during the collision of the striker with the test piece the Mach number, through the relation (5), determines how far the shock wave propagates up to the time when the relaxation wave reaches it; i.e., in other words it determines the permissible value of the base line for measuring D. In its turn, $\tan\alpha$ imposes conditions on the ratio between the diameter of the test sample d and its height h. In order to preserve a region near the axis of the sample cylinder which is not affected by lateral relaxation, where the shock wave parameters can be measured, the condition

$$d > 2h\ \tan\alpha^*$$

must be fulfilled.

For high degrees of compression and correspondingly high pressures, the amplitude of the relaxation shock wave becomes negligibly small in comparison with the pressures under study. This permits the use of the values M and $\tan\alpha$ in place of M* and $\tan\alpha^*$ in calculating sample dimensions. The above considerations were taken into account in setting up the experiments whose results are given in references 1 and 2.

5. THE ISENTROPIC COMPRESSIBILITY OF METALS

Let us generalize the results so far obtained by expressing the modulus of isentropic compression in the form of a power series:

$$K_s = \rho_0 C_\Gamma^2 = \sum_{k=1}^{n} b_k(\sigma-1)^{k-1}. \tag{7}$$

Integrating (7) leads to the function

$$I(\sigma) = \sum_{k=1}^{n} b_k k^{-1}(\sigma-1)^k. \tag{8}$$

At $P = 0$ and $\sigma = 1$, $I(\sigma)$ has a contact of the third order with the isentropic which passes through the origin of coordinates, and a second order contact with the Hugoniot adiabat. This circumstance determines the relations between the first three coefficients of (8) and the coefficients in the expression for the dynamic adiabatic:

$$P_\Gamma = \sum_{k=1}^{n} a_k(\sigma-1)^k.$$

It is easy to show that $b_1 = a_1$, $b_2 = 2a_2$, and $b_3 = 3a_3 - \frac{1}{2}\gamma_{p0}(a_1 + a_2)$, where γ_{p0} is the value of the Grüneisen coefficient for the lattice under nor-

TABLE V

Metal	b_k, 10^{10} d/cm²					
	k=1	2	3	4	5	6
Aluminum	73.1	305.4	194.8	—444	519	—106
Copper	137.0	543.4	266.8	4037	—11745	9650
Lead	41.4	203.4	184.2	248	—439	167
Iron	196.3	—157.0	3862.2	—5448	3077	—

mal conditions (P = 0; T = 20° C). The values of the coefficients a_1, a_2, and a_3 are borrowed from reference 6. For aluminum, copper, and lead γ_{p0} is taken equal to 2.09, 1.98, and 2.46 respectively. The coefficients b_4, b_5, and b_6 are chosen to fit the experimental data. The numerical values of the coefficients are shown in Table V. For iron, the chosen coefficients determine the isentropic modulus in the interval $1.20 < \sigma < 1.8$. These coefficients are not related to the parameters of iron under the initial conditions, since at $\sigma = 1.22$, according to Bancroft[2] there is a break in the compressibility curve caused by a phase transition.

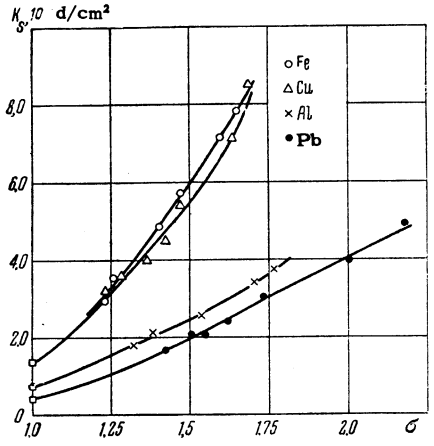

FIG. 8. Dependence of isentropic compression modulus K_S on the degree of compression. □ – initial value of $K_S = \rho_0 C_0^2$.

Figure 8 shows the variation of the isentropic modulus with the degree of shock compression. The isentropic modulus increases rapidly with the amplitude of the shock wave. Thus, for lead at $\sigma = 2.1$ and $P_\Gamma = 3.2 \times 10^{12}$ d/cm² it exceeds its initial value by more than ten times.

The experimental dependence of the speed of sound $C_\Gamma = \sqrt{K_S/\rho_0}$ on the degree of shock compression is shown in the left-hand side of Table VI for the four metals under investigation.

6. UPPER LIMIT OF THE CURVES OF "COLD" COMPRESSION. ESTIMATES OF THERMAL ENERGIES AND TEMPERATURES

Let us assume that the total pressure is the sum of the "cold" and thermal pressures: $P_\Gamma = P_X + P_T$. Inasmuch as $(\partial P_T/\partial \rho)_S > 0$, it is possible to establish unconditionally that $C_X^2(\sigma) < C_\Gamma^2(\sigma, T)$, where $C_X(\sigma)$ is the speed of sound at T = 0. Hence it follows that

$$P_X(\sigma) < \int_{\sigma_k}^{\sigma} \rho_0 C_\Gamma^2 d\sigma = I(\sigma) - I(\sigma_k) = I(\sigma, \sigma_k), \qquad (9)$$

where $\sigma_k = \rho/\rho_k$, and ρ_k is the density of the material at T = 0° K and P = 0. Thus the function $I(\sigma, \sigma_k)$ appears as the upper limit of the possible positions of the cold compression curve. The relative positions of the dynamic adiabatic, the function $I(\sigma, \sigma_k)$, and the cold compression curve $P_X(\sigma)$ taken from reference 6, are illustrated in Figs. 9 and 10. Comparison shows that the curves $P_X(\sigma)$ are located below $I(\sigma, \sigma_k)$, in agreement with the above. It is characteristic of all the metals that $I(\sigma, \sigma_k)$ is considerably closer to $P_X(\sigma)$ than to P_Γ. The presence of a difference $P_\Gamma - I(\sigma, \sigma_k)$ was the first experimental evidence, ten years ago, of the large part played by thermal pressure in the shock compression of solid bodies.

TABLE VI

σ	C_Γ (km/sec) from ref. 7				C_Γ (km/sec), calculated[6]		
	Al	Cu	Pb	Fe	Al	Cu	Pb
1.1	6.23	4.70	2.37		6.16	4.67	2.34
1.2	7.17	5.53	2.83		7.04	5.46	2.80
1.3	8.03	6.36	3.29	6.91	7.87	6.21	3.24
1.4	8.81	7.12	3.74	7.83	8.67	6.98	3.70
1.5	9.57	7.83	4.18	8.70	9.52	7.80	4.15
1.6	10.34	8.59	4.60	9.54	10.31	8.73	4.60
1.7	11.10	9.67	4.98	10.40	11.04	9.80	4.98
1.8			5.34				5.32
1.9			5.67				5.58
2.0			5.98				5.82
2.1			6.26				6.13

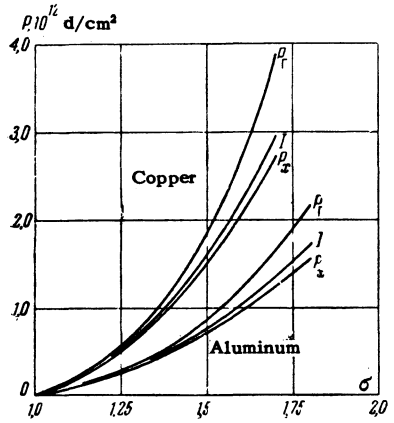

FIG. 9

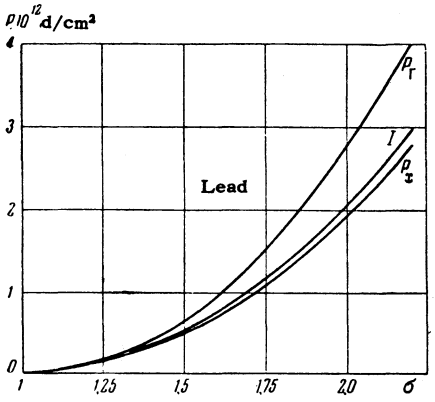

FIG. 10

The thermal energy of the shock compression is

$$E_T - E_0 = \tfrac{1}{2} P_\Gamma (\sigma - 1)/\rho_0\sigma - \int_{\sigma_K}^{\sigma} (P_x/\rho_0\sigma^2)d\sigma. \quad (10)$$

Let us find the lower bound of the value $E_T - E_0$, by replacing P_x in the integrand of (10) by the function $I(\sigma, \sigma_k)$, considered as a first approximation to $P_x(\sigma)$. The thermal energies calculated in this way are shown in Table VII. They are very close to the true values, since for small degrees of compression P_Γ, P_x, and $I(\sigma, \sigma_k)$ are close together, while at high compressions the major role in (10) is played by the first term, with the result that the relative error due to the substitution of the function $I(\sigma, \sigma_k)$ for the true curve $P_x(\sigma)$ is very small. It should be emphasized that the upper limit of the position of the compression curve at the absolute zero of temperature and the values of the thermal energy have been obtained directly from experimental measurements of the dynamic and isentropic compressibilities, without appealing to any one form or another of the equation of state.

Assuming the specific heat of the metals to be of the form $C_V = C_{Vp} + \beta T$ (C_{Vp} being the specific heat of the lattice, and βT the electronic specific heat), then by solving the equation

$$E_T = E_0 + C_{vp}(T - T_0) + \tfrac{1}{2}\beta T^2/2 \quad (11)$$

it is possible to calculate the temperature of the shock compression to the same degree of approxi-

TABLE VII

σ	1.1	1.2	1.3	1.4	1.5	1.6	1.7	1.8	1.9	2.0	2.1
Aluminum											
$E_T - E_0$, 10^{10} erg/g	0.043	0.164	0.449	1.027	2.086	3.817	6.331	9.616			
T, 10^3 deg K	0.34	0.48	0.78	1.40	2.46	4.18	6.47	9.25			
T from ref. 6, 10^3 °K	0.35	0.49	0.82	1.48	2.64	4.41	6.79	9.67			
γ_p					1.1	1.1	1.1	1.1			
γ_p from ref. 6					1.44	1.43	1.39	1.30			
Copper											
$E_T - E_0$, 10^{10} erg/g	0.026	0.103	0.315	0.752	1.514	2.882	5.069				
T, 10^3 deg K	0.36	0.56	1.11	2.20	4.29	7.24	11.97				
T from ref. 6, 10^3 °K	0.36	0.58	1.15	2.30	4.35	7.53	12.42				
γ_p					1.2	1.2	1.2				
γ_p from ref. 6					1.55	1.53	1.54				
Lead											
$E_T - E_0$, 10^{10} erg/g	0.042	0.067	0.127	0.265	0.505	0.884	1.432	2.139	3.005	3.985	5.138
T, 10^3 deg K	0.36	0.55	0.99	1.92	3.43	5.54	8.23	11.30	14.64	18.05	21.70
T from ref. 6, 10^3 °K	0.36	0.56	1.04	2.00	3.55	5.73	8.48	11.59	15.00	18.47	22.15
γ_p					1.5	1.4	1.3	1.25	1.15	1.0	0.9
γ_p from ref. 6					1.77	1.69	1.60	1.48	1.35	1.21	1.07

mation.* As can be seen from Table VII, the temperatures calculated in this way differ very little from the temperatures obtained in reference 6.

Replacing P_x by $I(\sigma, \sigma_k)$ makes it possible also to obtain a lower limit for the values of the Grüneisen coefficients, if the pressures on the Hugoniot adiabatic and the shock wave temperatures T, found above, are substituted into the equation for the dynamic adiabat:[6]

$$P_\Gamma = P_x + \rho_0\sigma C_{vp}\gamma_p [T - T_0 + E_0/C_{vp}] + \tfrac{1}{4}\rho_0\sigma\beta T^2. \quad (12)$$

Equation (12), apart from quantities which have already been mentioned, involves the quantities $\beta = \beta_0\sigma^{1/2}$, β_0 being the coefficient of electronic specific heat at $\sigma = 1$, and T_0 and E_0 being the temperature and internal energy under normal conditions. The observed γ_p are about 20 — 25% smaller than the values calculated in reference 6 (see Table VII).

Finally, let us use the measured sound velocity data, and the approximate values of T and γ_p which have been obtained, to determine the slopes of the dynamic adiabats. To this end we write the expression for the sound velocity at the Hugoniot adiabat:

$$\rho_0 C_\Gamma^2 = \frac{dP_x}{d\sigma} + \left[1 + \frac{d\ln\gamma_p}{d\ln\sigma} + \frac{C_{vp}\gamma_p}{C_{vp}+\beta T}\right]\rho_0 C_{vp}\gamma_p T + \frac{1}{2}\left[\frac{4\gamma_p C_{vp}+\beta T}{C_{vp}+\beta T} + \frac{1}{2}\right]\rho_0\beta T^2. \quad (13)$$

Differentiating (12) and eliminating $dP_x/d\sigma$ with the aid of (13), we arrive at the relation†

$$\frac{dP_\Gamma}{d\sigma} = \frac{\rho_0 C_\Gamma^2 - (P_\Gamma/2\sigma)[\gamma_p(1-\beta T/C_{vp}) + \beta T/2C_{vp}]}{1-(\sigma-1)[\gamma_p(1-\beta T/C_{vp}) + \beta T/2C_{vp}]/2}. \quad (14)$$

An estimate of $dP_\Gamma/d\sigma$ with the aid of the approximate values of T and γ_p by means of (14) is considerably more accurate than an estimate from the results of dynamic measurements because of the inevitable inaccuracies in recording the coordinates, which are sufficiently trustworthy to fix the location of the Hugoniot adiabat in the field of the P, σ diagram, but not its slope. In deriving the equation of state for the high pressure region, the original experimental data in references 6 and 8 are the results of dynamic compressibility measurements, in the form of an equation for the dynamic adiabatic $P_\Gamma = \sum_{k=1}^{n} a_k(\sigma-1)^k$. The equation of state obtained by this method, according to (14), can represent the actual slope of the isentropic correctly only in case the original analytical expression for the Hugoniot adiabatic describes the true values of the derivatives with sufficient accuracy over the entire length of the adiabat. Taking this fact into account made it possible to obtain, in reference 6, an equation of state suitable for calculating the speed of sound. As Table VI shows, the discrepancy between the experimental and calculated values of C_Γ does not exceed 2%.

The present work was begun under the initiative of Academician Ya. B. Zel'dovich in 1948. A number of valuable proposals were made by Corresponding Member of the Academy of Sciences (U.S.S.R.) E. I. Zababakhin. K. K. Krupnikov, B. N. Ledenev, and A. A. Bakanova contributed to the success of the investigation by their studies on the shock compression of metals, and also by taking part in the discussions. The authors received assistance on questions of apparatus and methods from Prof. V. A. Tsukerman and his coworkers, I. Sh. Model' and M. A. Kanunov. Individual measurements which contributed to the work were obtained by V. I. Borodulin. In carrying out the experiments, N. S. Tenigin, A. N. Kolesnikova, L. N. Gorelova, and M. S. Shvetsov took part, along with the authors.

To all these comrades the authors express their profound gratitude.

*In these calculations we have used the values given in reference 6 for E_0, T_0, C_{vp}, and β.

†The derivation of (14) given here is due to Yu. M. Shustov; in its general form, the relation between the Grüneisen coefficient and the derivatives of the two intersecting curves in the field of the P-ρ diagrams was previously given by K. K. Krupnikov.

[1] Al'tshuler, Krupnikov, Ledenev, Zhuchikhin, and Brazhnik, JETP **34**, 874 (1958), Soviet Phys. JETP **7**, 606 (1958).

[2] Al'tshuler, Krupnikov, and Brazhnik, JETP **34**, 886 (1958), Soviet Phys. JETP **7**, 614 (1958).

[3] A. S. Dubovik, Ж. научн. прикл. фотогр. и кинематогр. (J. Sci. and Appl. Photogr. and Cinematog.) **2**, 293 (1957).

[4] J. J. Gilvarry, Phys. Rev. **102**, 317 (1956).

[5] P. V. Bridgman, Study of Large Plastic Deformations and Rupture (Russ. transl.) IIL (1955).

[6] Al'tshuler, Kormer, Bakanova, and Trunin, JETP **38**, 790 (1960), Soviet Phys. JETP **11**, 573 (1960).

[7] Bankroft, Peterson, and Minshall, J. Appl. Phys. **27**, 291 (1956).

[8] Walsh, Rice, McQueen, and Yarger, Phys. Rev. **108**, 196 (1957).

Translated by D. C. West
213